CI&CEQ
Chemical Industry & Chemical Engineering Quarterly

Available online at
Association of the Chemical Engineers of Serbia AChE
www.ache.org.rs/CICEQ

Chem. Ind. Chem. Eng. Q. 32 (4) xxx–xxx (2026) CI&CEQ

SRINIVASAN PERIASAMY MANIKANDAN
http://orcid.org/0000-0003-0506-7282
JAYABALAN JAYABHARATHI
http://orcid.org/0000-0003-3747-5926

Department of Chemical Engineering, Kongu Engineering College, India

EXPERIMENTAL STUDIES USING NON - NEWTONIAN NANOFLUID OF SiO_2-WATER-EUTECTIC SOLVENT IN A PLATE HEAT EXCHANGER

Highlights

- Performance of eutectic solvent-water as a base fluid in a plate heat exchanger was assessed.
- The heat transfer performance of the SiO_2 suspended base fluid was studied in a plate heat exchanger.
- Individual and overall heat transfer coefficients were determined and analyzed by varying the flow rate.

Abstract

The plate heat exchanger is one of the smallest and most efficient heat exchangers on the market. This experiment aims to assess the performance of eutectic solvent-water as a base fluid in a plate heat exchanger. For this study, silicon oxide (SiO_2) nanoparticles are synthesized from sugar bagasse and rice husk, using the sol-gel method. SiO_2 nanoparticles were used in various ratios (0.15 vol.%, 0.3 vol.%, 0.45 vol.%, 0.6 vol.%, and 0.75 vol.%) in a base fluid (15 vol.% eutectic solvent and 85 vol.% water) to prepare a nanofluid. At three different temperatures, such as 323 and 343 K, with varying flow rates (2-8 L/min) and varying nanoparticle concentrations (0.15 % to 0.75 %), heat transfer studies were performed, and the results are presented. There was a notable enhancement in the overall heat transfer coefficient by the combination of SiO_2 nanoparticles and an eutectic solvent-water-based fluid. It was noted that utilizing the SiO_2/eutectic solvent-water nanofluid could significantly reduce the temperature gradient in the heat exchanger and improve its performance. The maximum overall heat transfer coefficient noted was 3162.5 W/m²K at 0.6 % volume fraction of nanoparticles, with a flow rate of 8 L/min at a temperature of 343 K.

Keywords: base fluid, eutectic solvent, heat transfer, non-Newtonian nanofluid, plate heat exchanger, SiO_2.

SCIENTIFIC PAPER

UDC

INTRODUCTION

Silica (SiO_2) has numerous useful properties, such as tunable pore dimensions, customizable surface properties, and chemically stable composition, making it ideal for improving heat transfer and applications in the medical industry, and its non-toxic nature [1,2]. Of these, sugarcane bagasse and rice husk/straw are particularly valuable due to their high silicon content. They are important renewable resources [3,4]. These studies suggest exciting possibilities for extracting silica from agricultural waste. Numerous studies explore creating silica nanoparticles using organic compounds and diverse techniques [5,6]. Different strategies have been created for silica nanoparticle blends, utilizing both bottom-up and top-down procedures [7]. The sol-gel strategy is the most common way to form silica nanoparticles since it can make uniform nanoparticles with a limited measure of conveyance beneath mellow conditions [8]. The conversion of ash to silica gel starts with reacting ash with caustic lye to produce sodium silicate, as follows:

$$SiO_2 + 2NaOH \rightarrow Na_2SiO_3 + H_2O \quad (1)$$

It is achieved by precipitating silica gel through the reaction of sodium silicate with hydrochloric acid:

$$Na_2SiO_3 + 2HCl \rightarrow SiO_2 + 2NaCl + H_2O \quad (2)$$

The purification and drying process produces amorphous silica powder, eliminating impurities or organic matter commonly present in the waste [9].

Correspondence: P.M. Srinivasan, Department of Chemical Engineering, Kongu Engineering College, Erode-638 060, India.
Email: sriperiasamy@gmail.com
Paper received: 7 July 2025
Paper revised: 22 December 2025
Paper accepted: 4 February 2026

https://doi.org/10.2298/CICEQ250707001M

These papers mainly focus on the numerical study of the heat transfer performance of nanofluids in heat exchangers. The nanoparticles studied include titanium oxide, silicon oxide, graphene oxide, aluminum oxide, and zinc oxide. Most studies vary the nanoparticle concentration and flow rate [10–12]. They often use base liquids such as ethylene glycol, glycerol, motor oil, and water. Some papers also focus on the shape of the nanoparticles [13,14]. This study assessed the heat transfer performance of SiO_2-water nanofluids. The convective heat transfer coefficients were analyzed for SiO_2-water nanofluids with varying particle sizes. The influence of particle size and Reynolds number (Re) on the heat transfer coefficients was examined. The findings reveal that both the particle size of SiO_2 nanoparticles and the Reynolds number play a significant role in determining the convective heat transfer coefficient. Incorporating SiO_2 nanoparticles with sizes of 15 nm, 30 nm, and 80 nm into water enhanced the nanofluid's convective heat transfer coefficient by up to 36.8 % [15]. Water, ethylene glycol, glycerol, and engine oil demonstra-te relatively high thermal conductivities and specific heats, but their boiling points and melting points restrict their utilization in high-temperature and very low temperature application. For example, temperatures in the summer of countries near the equator can reach up to 333 K, while in the winter, temperatures in northern Canada can drop to 233 K. Therefore, a working fluid that can withstand such large temperature differences is highly desirable. Traditi-onally, base solvents for nanofluids are classified into water, liquor, and mineral oil. These dissolvable frameworks regularly endure from either a generally limited fluid extent or poor thermal stability [16,17]. To address this issue, DES has risen as a promising elective due to its low vapor pressure and high boiling point [18,19].

DESs, also known as ionic liquid analogues, are a class of solvents consisting of a mixture that creates a eutectic system with a significantly lower melting point than any of its individual components [20]. The thermal conductivities of seven choline chloride-based DESs, like reline, tegaline, maline, glyceline, ethaline, glucoline, and fructoline, have been documented across the temperature range of 298 K to 363 K [21]. Glyceline is favored for its good thermal conductivity, low viscosity, and exceptional thermal stability, making it a more efficient option for heat transfer applications compared to other choline chloride-based DES [22]. The expansion of 75 wt% water comes about in about three times higher thermal conductivities in all DES [23]. Rashmi Walvekar *et al.* [24] conducted heat transfer studies with DES-CNT-nanofluids and found to increase the thermal stability of ethylene glycol and triethylene glycol (TEG) because of the lower freezing points (down to -117.90 °C) of eutectic solvents as compared to EG and TEG. Wei Shi *et al.* [25] measured and analyzed the effects of the SiO_2, TiO_2, and Al_2O_3 nanoparticles and temperature on the density and viscosity of choline chloride/ethylene glycol deep eutectic solvent-based nanofluids. Yu Yan *et al.* [26] prepared super-stable copper oxide/DES nanofluids and comprehensively studied the thermophysical and photo-thermal characteristics of the prepared nanofluids. Indradeep *et al.* [27] used an engine oil containing nanoparticles of SiO_2 to studythe heat transfer performance of double-pipe exchangers and reported a16 % improvement in the Nusselt numberat a 0.2 % concentration. Vijayakumar *et al.* [28] observed that the thermal quality of the cotton-seed oil-blended diesel was significantly enhanced with the diffusion of nano-MgO.

Despite the numerous advantages of using nanofluids, there are also some disadvantages, such as limited boiling points and melting points that restrict their use in high temperature and very low-temperature applications, surface erosion, and instability. When dispersing nanoparticles in a base fluid, a choline chloride/glycerol mixture offers both high- and low-temperature applications. Choline chloride, being an ionic salt, provides good thermal conductivity and is non-toxic. Compact plate heat exchangers were selected for our study, as existing research highlights their efficiency and superior performance when used with nanofluids. However, the heat transfer behavior of a nanofluid blend comprising SiO_2, choline chloride, glycerol, and water in a plate heat exchanger remains unexplored in the literature. Also, we have included the studies on the non-Newtonian behavior of prepared nanoparticles, which is critical for energy saving. Since plate heat exchangers are applied for heating, cooling, evaporation, and condensation of various chemicals, solvents, and pharmaceutical liquids, with a typical operating temperature range from about 243 K up to 473 K. In the present study, an average temperature between 323, 333, and 343 K was selected, while the flow rates were varied.

MATERIALS AND METHODS

Materials

Sugar bagasse and rice husk were used as raw materials, collected from a nearby agricultural area. Analytical-grade reagents, including sodium hydroxide and hydrochloric acid, were employed without further purification. Silicon nanoparticles were synthesized using sugar bagasse and rice husk ash through the sol-gel technique. Distilled water was used consistently throughout the experiment.

Preparation of ash

Sugar bagasse and rice husk were gathered and rinsed with distilled water to eliminate dust and soil particles. Following the cleaning process, the sugar bagasse and rice husk were dried in an oven at 343 K for 24 hours. The dried materials were then incinerated in a muffle furnace at 973 K for 2 hours to remove all embedded organic compounds.

Silica preparation

After preparing the sugar bagasse and rice husk ash, take 100 g of ash and mix it with 1 liter of 2N sodium hydroxide. The mixture was stirred by a magnetic stirrer at a constant rpm for 2 hours, maintaining the temperature at 358 K. The filtrate from the sodium silicate arrangement was cooled to room temperature. The mixture of sugar bagasse and rice husk ash with NaOH formed a sodium silicate solution. Filter paper was used to collect the sodium

silicate solution, then 2N HCl was added dropwise until the pH reached 7. Once the pH reached 7, the solution was cooledto room temperature and stood for 24 hours to form the silica gel. After gel formation, it was rinsedwith deionized water to eliminate minerals and impurities. Finally, the gel was dried in an oven at 363 K for 48 hours to produce silica nanoparticles. Sugar bagasse is a widely available by-product of sugar processing and silica-rich feedstock with potential purity, whereas rice husk-derived SiO_2 nanoparticles offer strong waste valorization potential. Since both sugar bagasse and rice husk are by-products of widely grown crops, generating large volumes of silica content and available at low material cost, this reduces the overall SiO_2 nanoparticle production cost.

Characterization of Silica Nanoparticles

Fourier Transform Infra-Red spectroscopy

Fourier transform infra-red (FTIR) spectra were used to investigate the structure and identify functional groups. Figure 1 illustrates the FTIR spectra of silica nanoparticles synthesized from (a) sugar bagasse and (b) rice husk. The FTIR spectra of the adsorbents were acquired using an IR tracer, covering the range from 400 to 4000 cm^{-1}. Notably, the Si-O-Si vibration peak is observed in both types.

(a) SiO_2 nanoparticles synthesized from sugar bagasse

The Si-O-Si transmittance peaks were assigned to twisting, asymmetric stretching, and symmetric balanced stretching at 408 cm^{-1}, 439 cm^{-1}, 493 cm^{-1}, 540 cm^{-1}, 601 cm^{-1}, 671 cm^{-1}, 686 cm^{-1}, and 1087 cm^{-1}, respectively [10]. The silica surfaces displayed a wide peak at 3402 cm^{-1}, attributed to hydroxyl extending vibrations caused by residual adsorbed water and the vibration of the silanol bunch [25]. The band near 1643.35 cm^{-1} could be assigned to the bending of the H-O-H bond in water molecules [26].

(b) SiO_2 nanoparticles synthesized from rice husk

The Si-O-Si transmittance peaks were assigned to the twisting, asymmetric stretching, and symmetric balanced stretching at 424 cm^{-1}, 439 cm^{-1}, 478 cm^{-1}, 601 cm^{-1}, 671 cm^{-1}, 871 cm^{-1}, 1049 cm^{-1}, and 1095 cm^{-1} respectively [10]. The silica surfaces displayed a wide peak at 3410 cm^{-1}, assigned to hydroxyl extending vibrations caused by residual adsorbed water and the vibration of the silanol bunch. The band near 1643 cm^{-1} can be assigned to the bending of the H-O-H bond in water molecules.

Scanning electron microscope analysis

Scanning electron microscopy (SEM) is widely employed for analyzing the surface microstructure and chemical properties of materials. It uses a concentrated electron beam to scan the surface and generate an image. The interaction between the electron beam and the sample produces various signals, which are utilized to obtain information about the surface composition.

(a) SiO_2 nanoparticles synthesized from sugar bagasse

Figure 2(a) shows the SEM analysis of SiO_2 nanoparticles synthesized from sugarcane bagasse. The image gives an intense structure of elongated, needle-like microstructures spread across the surface and having sizes between about 100 and 140 nm. The material appears to be highly porous, granular, and agglomerated with a broad distribution of particle sizes. Regions of agglomerated particles possess irregularity in surface smoothness and homogeneity compared to the regions where particles were well spread out. The feature size in the agglomerated region is larger than that in the non-agglomerated regions.

(b) SiO_2 nanoparticles synthesized from rice husk

Figure 2(b) shows an SEM analysis of SiO_2 nanoparticles prepared from rice husk. The picture contains well-defined edged structures that represent crystalline structures scattered all over the surface, with some irregularly shaped particles. It varies in size between 80 and 90 nm. The uniformity in these particle sizes indicates a controlled process of synthesis or deposition. Mixed morphology, with smaller and larger particles, provides a balance between reactivity and structural strength.

Energy dispersive X-ray analysis

Energy dispersive X-ray (EDX) spectroscopy is an analytical technique for determining the composition of materials in elemental terms.

(a) EDX analysis of SiO_2 nanoparticles synthesized from sugarcane bagasse

Figure 3(a) shows the EDS analysis of SiO_2 nanoparticles synthesized from sugarcane bagasse. The image displays a prominent silicon oxide peak; however, some impurities such as sodium (Na) and chloride (Cl) are also present. This indicates surface contamination by salts.

(b) EDX analysis of SiO_2 nanoparticles synthesized from rice husk

Figure 3(b) presents the EDS analysis of SiO_2 nanoparticles synthesized from rice husk. The image reveals a clear silicon oxide peak, indicating the presence of primarily silicon, oxygen, and trace amounts of carbon. This composition suggests a purer form of the material compared to the nanoparticles synthesized from sugarcane bagasse.

Selection of nanoparticles

Silica nanoparticles will be synthesized from both sugarcane bagasse and rice husk. Compared to silica derived from rice husk, the silica obtained from sugarcane bagasse contains impurities such as sodium (Na) and chloride (Cl), while silica derived from rice husk is of higher purity compared to silica derived from sugarcane bagasse. In this paper, SiO_2 nanoparticles were synthesized from rice husk to prepare a nanofluid for the study of heat transfer performance.

Preparation of nanofluid and non-Newtonian behaviour

SiO_2 nanoparticles of 90 nm size were dispersed using a two-step sol-gel process in the eutectic solvent mixture with water. Base fluids with volume fractions of 15 %

.

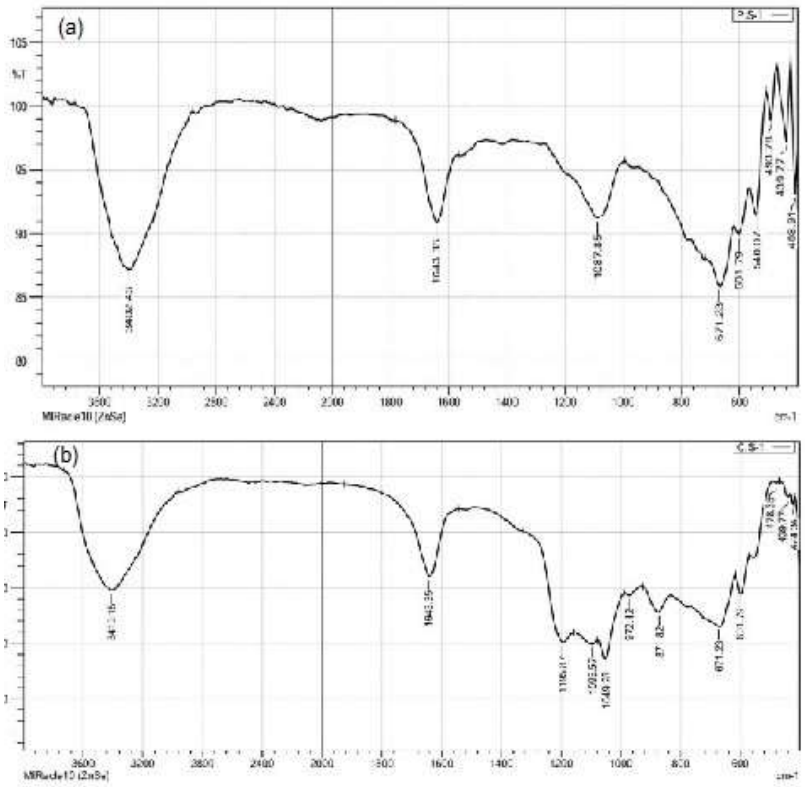

Figure 1. FT-IR spectra of SiO_2 nanoparticles synthesized from (a) sugarcane bagasse and (b) rice husk.

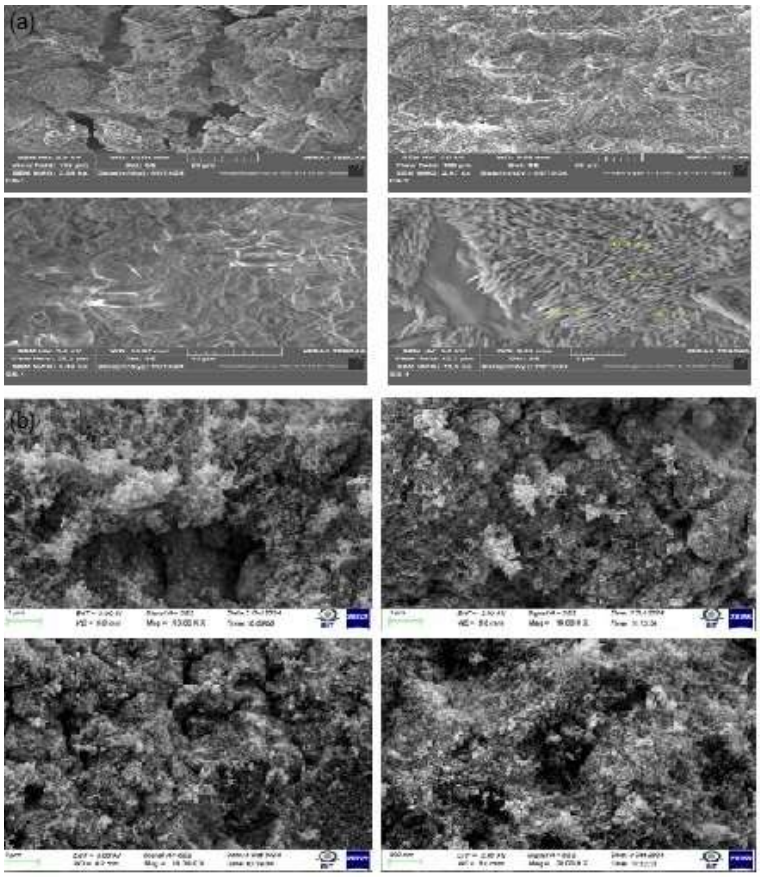

Figure 2. SEM analysis showing of surface morphology at different magnifications, microstructural evolution and porosity characteristics for SiO_2 nanoparticles synthesized from (a) sugarcane bagasse and (b) rice husk.

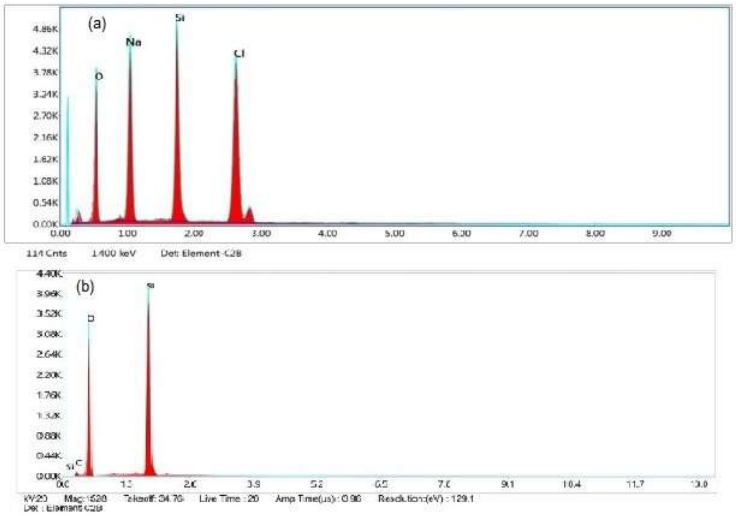

Figure 3. EDX analysis of SiO_2 nanoparticles synthesized from (a) sugarcane bagasse and (b) rice husk.

eutectic mixture and 85 % water were prepared using the amounts calculated from Eq. (3)

$$\varphi = \frac{(m/\rho)_{\mathrm{SiO_2}}}{(m/\rho)_{\mathrm{SiO_2}} + (m/\rho)_{\mathrm{W:ES}}} \qquad (3)$$

where φ is the nanoparticle volume fraction, dimensionless, m is the mass, and ρ is the density.

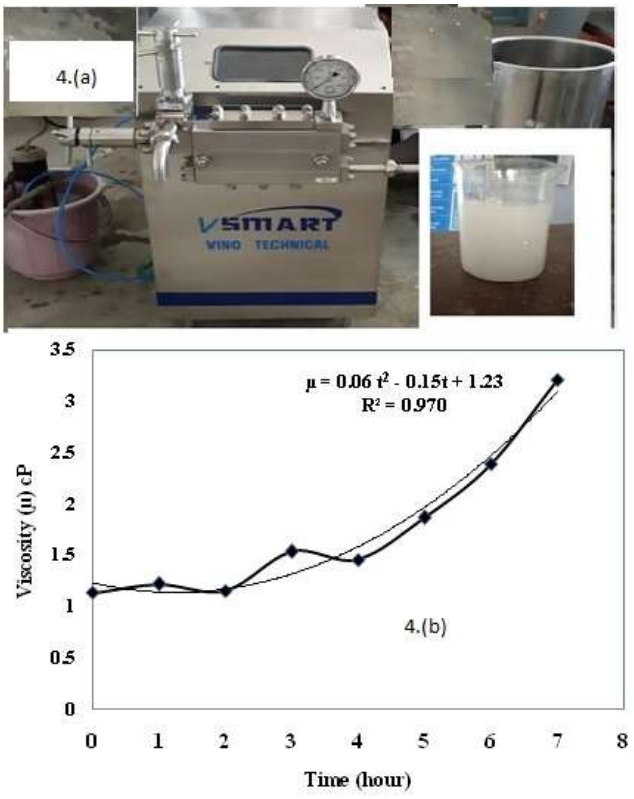

Figure 4. High pressure homogenizer and prepared nanofluid (b) Change in viscosity of fluid with time in the homogenizer, during the synthesis of nanoparticles.

A major limitation in the preparation of nanofluid is its stability over a period of experimentation, since these particles tend to clump together over time. Preparation includes instability, where nanoparticles clump together over time, which also requires more power to pump these fluids. To overcome this challenge, a stable nanofluid was prepared using a high-pressure homogenizer. The stability achieved is attributed to effective particle dispersion under high shear conditions, accompanied by time-dependent changes in fluid viscosity during homogenization. The preparation of nanofluid and evolution of viscosity during nanofluid synthesis is presented in Figures 4(a) and (b). Prepared nanofluid is homogeneously suspended throughout the base fluid because of high pressure homogenizer.

The use of the high-pressure homogenizer, shown in Figure 4(a), ensured a uniform suspension of nanoparticles within the base fluid. In order to assure stability in the prepared nanofluid, a high-pressure homogenizer was applied, and the prepared nanofluid was used in the plate heat exchanger as cold fluid. It was noted that the particles are homogeneously dispersed throughout the base fluid and ensured a good nanofluid suspension because of high pressurehomogenizer.

The nanoparticles, during their formation in a homogenizer, were tested for their rheological behaviour. Homogenizer was highly recommended for enhancing the mixing characteristics of non-Newtonian fluids. Hence, the viscosity of the solution was tested at regular time intervals and reported as shown in Figure 4(b). The fluid in the homogenizer was found to exhibit dialatant behaviour. The high gravitational field generated by centrifugal action of the rotating bed considerably increased the shear rate, facilitating enhanced molecular diffusion and contact among the reacting species [32]. It, in turn, increased the apparent viscosity of the fluid. The duration of shearing also increased the dynamic viscosity, exhibiting rheopectic behaviour. The viscosity values, as indicated in Figure 6, were changing with time as given by Eq. (4).

$$\mu = 0.06t^2 - 0.15t + 1.23 \qquad (4)$$

where μ is the viscosity of the nanofluid and t is time.

A polynomial fit (R^2 = 0.970) was more appropriate for depicting the change in viscosity with time. It was observed

that the viscosity increases with the increase in SiO_2 nanoparticle concentration, because viscosity is strongly influenced by the volume concentration of the nanoparticle. However, the magnitude of viscosity decreases with an increase in hot fluid inlet temperature.

Experimental setup

The experiments were conducted on a plate-type heat exchanger, where the hot and cold fluids flowed in a counter-current arrangement. Figure 4 displays a photograph of the experimental setup, which includes a plate heat exchanger, two reservoirs (for the hot and cold fluids), a temperature controller, flow meters for monitoring and regulating the flow, and two fluid pumps. The plate heat exchanger, as shown in Figure 5, consists of 13 corrugated stainless steel plates (Alfa Laval, India) with seven flow channels for the hot fluid and six for the cold fluid. The plate dimensions are 480 mm in length and 1 mm in thickness.

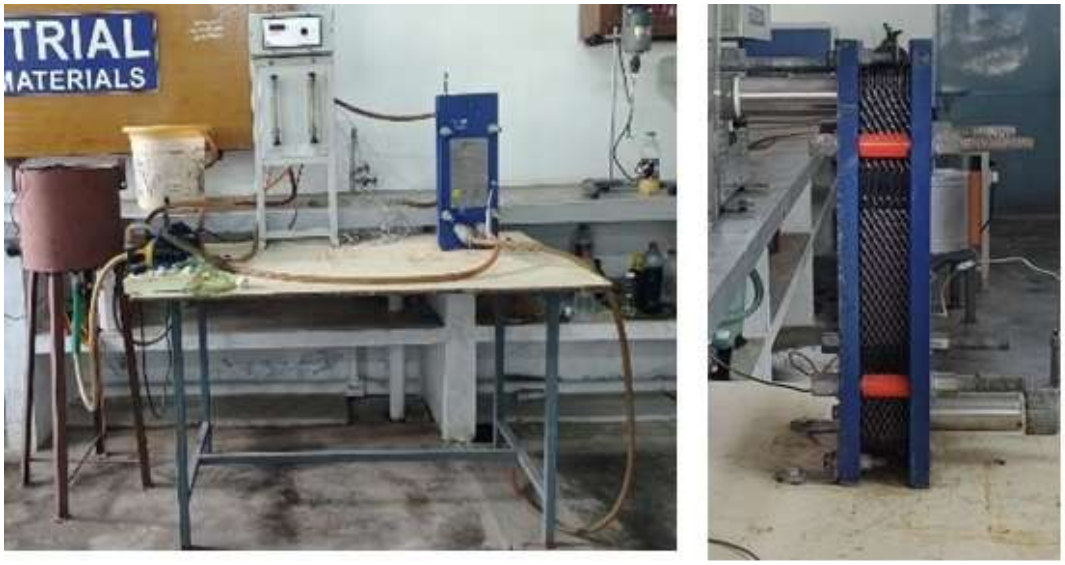

Figure 5. Photograph of experimental setup.

Determination of thermo-physical properties of nanofluid

Thermal conductivity was measured using a thermal conductivity analyzer (Scientico, India), and viscosity was measured with a redwood viscometer for all the concentrations of the mixture.

Density of nanofluid and specific heat capacity of nanofluid are calculated from the correlations [29-31] given in Eq.(5) and (6).

$$\rho_{nf} = (1-\varphi)\rho_{nf} + \varphi\rho_p \qquad (5)$$

where ρ_{hf} is the density of nanofluid (kg/m^3), and ρ_{hp} is the density of nanoparticles (kg/m^3).

$$Cp_{nf} = ((1-\varphi)\rho_{nf}Cp_f + \varphi\rho_p Cp_p)/(\rho_{nf}) \qquad (6)$$

where $C_{p.}$nf is the heat capacity of nanofluid (J/kgK), and $C_{p.p}$ is the heat capacity of nanoparticles (J/kgK).

The obtained results of thermo-physical properties were used for calculating different dimensionless numbers (Reynolds, Prandtl, and Nusselt numbers) applied in this study.

Determination of the Nusselt number and overall heat transfer coefficient of SiO_2-water eutectic solvent nanofluid

Eqs. (7) and (8) were used to determine the Nusselt number (Kim model) and heat transfer coefficient of the nanofluid:

$$Nu = 0.295(N\,\mathrm{Re})^{0.64}(N\,\mathrm{Pr})^{0.32}\left(\left(\frac{\pi}{2}-\beta\right)\right) \qquad (7)$$

$$U = Q \cdot A \cdot \Delta T_{LMTD} \qquad (8)$$

where Nu is the Nusselt number, Re is the Reynolds number, Pr is the Prandtl number, π is the mathematical constant, β is the corrugation angle, U is the overall heat transfer coefficient, Q is the heat flux, A is the area of a heat exchanger, and ΔT_{LMTD} is the logarithmic mean temperature difference.

RESULTS AND DISCUSSION

To evaluate the heat transfer properties of incorporating SiO_2 nanoparticles into a base fluid (eutectic solvent + water), the overall heat transfer coefficient (U) and rate of heat transfer were determined by adjusting the nanoparticle volume fraction (0.15 to 0.75 vol %), flow rate (2 to 8 L/min), and hot fluid inlet temperature (323 to 343 K) for a base fluid volume fraction of (15:85) (eutectic mixture:water).

Impact of flow rate and concentration on the overall heat transfer coefficient at 323 K

Figure 6 indicates that, for concentrations ranging from 0.15 to 0.75 vol.% at various flow rates (2-8 L/min) and a temperature of 323 K, the heat transfer coefficient shows significant variation. At a concentration of 0.15 vol.%, the heat transfer coefficient is 64.6 W/m²K at a flow rate of 2 L/min and increases to 474.2 W/m²K at a flow rate of 8 L/min. Similarly, at a concentration of 0.75 vol.%, the heat transfer coefficient is 262.3 W/m²K at a flow rate of 2 L/min and rises to 1410.5 W/m²K at 8 L/min. The maximum heat transfer coefficient at 323 K is 1645.8 W/m²K, achieved at a concentration of 0.6 vol.% and a flow rate of 8 L/min.

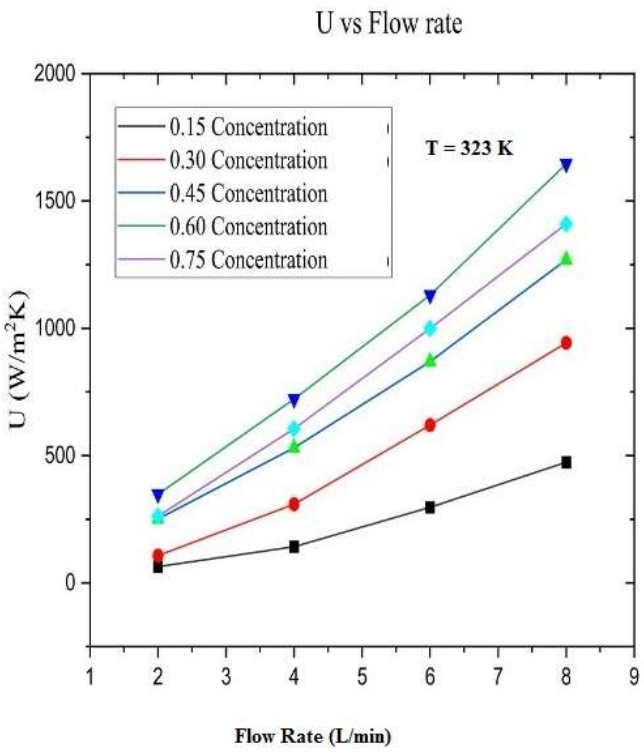

Figure 6. Impact of various flow rates and concentrations on the overallheat transfercoefficient (U) at a temperature of 323 K.

Impact of flow rate and concentration on the overall heat transfer coefficient (*U*) at 333 K

Figure 7 indicates that, for concentrations ranging from 0.15 to 0.75 vol.% at various flow rates (2-8 L/min) and a temperature of 333 K, the heat transfer coefficient exhibits significant variation.

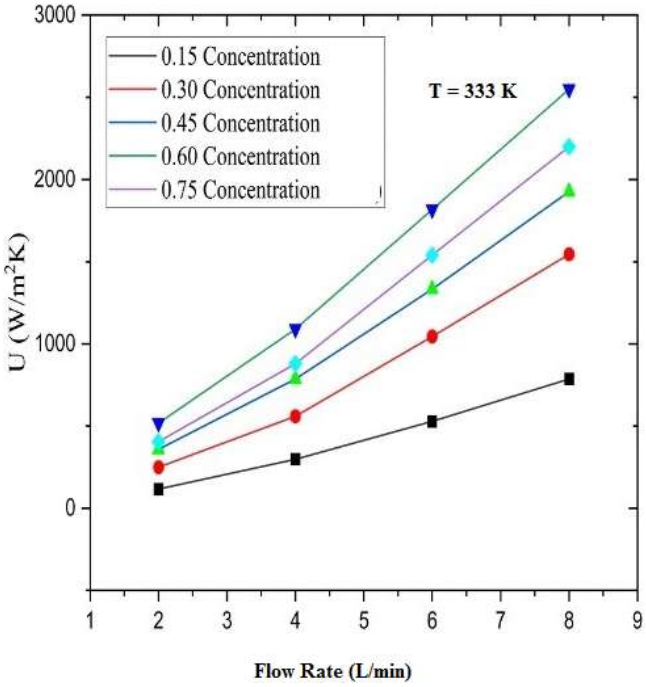

Figure 7. Impact of various flow rates and concentrations on the overall heat transfercoefficient (U) at a temperature of 333 K.

At a concentration of 0.15 vol.%, the heat transfer coefficient is 117.4 W/m²K at a flow rate of 2 L/min and increases to 786.8 W/m²K at a flow rate of 8 L/min. Similarly, at a concentration of 0.75 vol.%, the heat transfer coefficient is 404.9 W/m²K at a flow rate of 2 L/min and rises to 2200.1 W/m²K at 8 L/min. The maximum heat transfer coefficient at 333 K is 2549.1 W/m²K, achieved at a concentration of 0.6 vol.% and a flow rate of 8 L/min. These results further validate the ability of nanoparticle suspensions to significantly enhance heat transfer performance.

Impact of flow rate and concentration on the overall heat transfer coefficient at 343 K

Figure 8 indicates that, for concentrations ranging from 0.15 to 0.75 vol.% at various flow rates (2-8 L/min) and a temperature of 343 K, the heat transfer coefficient shows significant variation. At a concentration of 0.15 vol.%, the heat transfer coefficient is 169.41 W/m²K at a flow rate of 2 L/min and increases to 1289.41 W/m²K at a flow rate of 8 L/min. Similarly, at a concentration of 0.75 vol.%, the heat transfer coefficient is 538.55 W/m²K at a flow rate of 2 L/min and rises to 2683.46 W/m²K at 8 L/min. The maximum heat transfer coefficient at 343 K is 3162.43 W/m²K, achieved at a concentration of 0.6 vol.% and a flow rate of 8 L/min.Since the heat transfer coefficient is a measure of how effectively heat is transferred between a fluid and a surface through convection, by comparing the selected temperatures, the maximum enhancement of heat transfer is at 343 K.

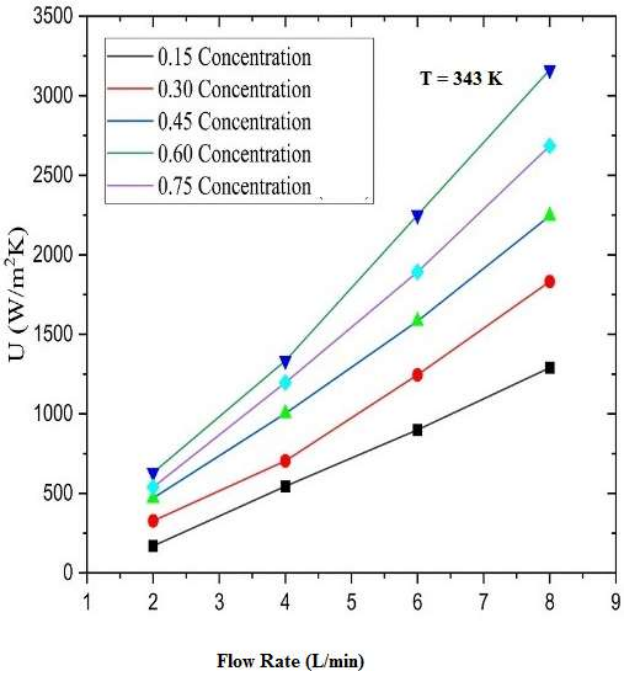

Figure 8. Impact of various flow rates and concentrations on the overall heat transfercoefficient (U) at a temperature of 343 K.

Based on the experimental results, the enhancement of the heat transfer coefficient with varying nanoparticle concentrations and flow rates at different temperatures can be summarized. In all three figures, the heat transfer coefficient increases with higher nanoparticle concentrations and higher flow rates. The impact of nanoparticle concentration is more significant at higher temperatures, with the maximum heat transfer coefficient consistently observed at an optimal concentration of 0.6 vol.% across all temperatures tested.

At a lower temperature (323 K), the increase in the heat transfer coefficient is moderate yet still significant, with the highest value achieved at the 0.6 vol.% concentration and the highest flow rate. As the temperature rises to 333 and 343 K, the enhancement in heat transfer becomes more pronounced. The maximum heat transfer coefficients at these higher temperatures are notably higher than at 323 K, especially at the same 0.6 vol.% concentration and flow rate.

In conclusion, the results from all three temperature conditions demonstrate that both nanoparticle concentration and flow rate play crucial roles in improving heat transfer performance. The greatest improvements in heat transfer are consistently achieved at a concentration of 0.6 vol.% and a flow rate of 8 L/min, irrespective of the temperature. This underscores the effectiveness of nanoparticle suspensions in enhancing heat transfer across various operating conditions.

CONCLUSION

The efficacy of a heat exchanger utilizing a combination of eutectic solvent, water, and SiO_2 nanoparticles was thoroughly examined under various flow rate and temperature conditions. Several key conclusions emerged from the study. First, the heat transfer coefficient increased with the concentration of SiO_2 nanoparticles in the nanofluid, with the highest efficiency observed at a concentration of 0.6 % at 343 K. Increasing nanoparticle volume fraction in all samples increases the overall heat transfer coefficient up to 0.6 vol.% after that the enhancement is decreasing, hence for a given set of operating parameters, an optimum enhancement was observed at 0.6 vol.% of SiO_2 nanoparticle volume fraction. Temperature was also a significant factor, as higher operating temperatures, particularly at 343 K, enhanced heat transfer performance by improving thermal conductivity. Moreover, increasing the flow rate of the nanofluid from 2 to 8 L/min resulted in a measurable improvement in the heat transfer coefficient, emphasizing the importance of fluid velocity for enhanced convective heat transfer. The stability of the nanofluid was maintained through the use of a high-pressure homogenizer, ensuring uniform dispersion of nanoparticles and preventing agglomeration, which is crucial for preserving the nanofluid's enhanced heat transfer properties over time. Overall, SiO_2 nanoparticle-based nanofluids outperformed traditional fluids, showing significant improvements in heat transfer efficiency, with optimal performance observed at 0.6 % nanoparticle concentration, beyond which the heat transfer performance decreased. These results help in the chemical, food, and pharmaceutical Industries which utilizes solvent as heat transfer fluids.

LIMITATIONS AND FUTURE WORK

It is suggested to study the heat transfer performance of the heat exchanger by considering the effect of experimental time on the results, since the nanofluid properties are affected by the running time in the system (mainly stability). Further heat transfer studies may be performed by combining different metal/metal oxide nanoparticle suspensions with different base fluids. In the future, studies with hybrid nanofluid (mixing different nanoparticles in the base fluid) can be explored and scaled up for industrial heat exchangers. It is also suggested to perform hydrodynamic and mass transfer behavior of a nanofluid with respect to Industrial applications.

ACKNOWLEDGMENT

The authors are grateful to Kongu Engineering College and the Department of Chemical Engineering for the facility provided.

NOMENCLATURE

Abbreviations

Al_2O_3	Aluminium oxide
CNT	Carbon Nano Tubes
DES	Deep eutectic solvent
EM	Eutectic mixture
PHE	Plate Heat Exchanger
SiO_2	Silicon oxide
TiO_2	Titanium dioxide
ZnO	Zinc oxide
ΔT_{LMTD}	Logarithmic mean temperature difference
W	Water
t	Time (hour)
wt%	Weight (%)
vol. %	Volume (%)
N_{Nu}	Nusselt number, dimensionless
N_{Pr}	Prandtl number, dimensionless
N_{Re}	Reynolds number, dimensionless

Symbols

Q	Heat flux, W
U	Overall heat transfer coefficient, (W/m^2 K)
$C_{p.nf}$	Heat capacity of nanofluid (J/kgK)
$C_{p.np}$	Heat capacity of nanoparticles (J/kgK)
$C_{p.bf}$	Heat capacity of base fluid (J/kgK)
φ	Nanoparticle volume fraction, dimensionless
ρ_{nf}	Density of nanofluid (kg/m^3)
ρ_{np}	Density of nanoparticles (kg/m^3)
ρ_{bf}	Density of base fluid (kg/m^3)
μ_{nf}	Viscosity of nanofluid (N·s/m^2)
μ_{bf}	Viscosity of base fluid (N·s/m^2)
k_{nf}	Thermal conductivity of nanofluid (W/mK)
k_{np}	Thermal conductivity of nanoparticles (W/mK)
k_{bf}	Thermal conductivity of base fluid (W/mK)

REFERENCES

[1] G.A. Seisenbaeva, L.M.A. Ali, A. Vardanyan, M. Gary-Bobo, T.M. Budnyak, V.G. Kessler, J.O. Durand, J. Hazard. Mater. 406 (2021)124698.https://doi.org/10.1016/j.jhazmat.2020.124698.

[2] L. Tang, J. Cheng, Nano Today 8 (2013) 290-312.https://doi.org/10.1016/j.nantod.2013.04.007.

[3] S.H. Javed, U. Aslam, M. Kazmi, M. Rustam, S. Riaz, Z. Munir, Pol. J. Chem. Technol. 17 (2015) 47-51. https://doi.org/10.1515/pjct-2015-0049.

[4] B. Rakesh, T. Chitdeshwari, S. Maragatham, D.J.S. Sharmila, A. Senthil, N. Chitra, Dig. J. Nanomater. Biostruct. 19 (2024) 605-618. https://doi.org/10.1016/j.stress.2024.100672
[5] H.B. Dizaji, T. Zeng, I. Hartmann, D. Enke, T. Schliermann, V. Lenz, M. Bidabadi, Appl. Sci. (Switz.) 9 (2019)4939. https://doi.org/10.3390/su14094939.
[6] S. Prabha, D. Durgalakshmi, S. Rajendran, E. Lichtfouse, Environ. Chem. Lett. 19 (2021) 1667-1691. https://doi.org/10.1007/s10311-020-01123-5.
[7] K.A.S. Usman, J.W. Maina, S. Seyedin, M.T. Conato, L.M. Payawan, L.F. Dumée, J.M. Razal, NPG Asia Mater. 12 (2020) 58. https://www.nature.com/articles/s41427-020-00240-5.
[8] I.A. Rahman, V. Padavettan, J. Nanomater. (2012)132424. http://doi.org/10.1155/2012/132424.
[9] A.B.D. Nandiyanto, T. Rahman, M.A. Fadhlulloh, A.G. Abdullah, I. Hamidah, B. Mulyanti, IOP Conf. Ser.: Mater. Sci. Eng. 128 (2016) 012040. https://doi.org/10.1088/1757-899X/128/1/012040.
[10] S.P. Manikandan, R. Baskar, Chem. Ind. Chem. Eng. Q. 24 (2018) 309-318. https://doi.org/10.2298/CICEQ170720003M.
[11] F. Garoosi, F. Hoseininejad, M.M. Rashidi, Appl. Therm. Eng. 105 (2016) 436-455. https://doi.org/10.1016/j.applthermaleng.2016.03.01.
[12] A.E. Kabeel, T. Abou El Maaty, Y. el Samadony, Appl. Therm. Eng. 52 (2013) 221-229. https://doi.org/10.1016/j.applthermaleng.2012.11.027
[13] J. Albadr, S. Tayal, M. Alasadi, Case Stud. Therm. Eng. 1 (2013) 38-44. https://doi.org/10.1016/j.csite.2013.08.004
[14] N. Kumar, S.S. Sonawane, Int. Commun. Heat Mass Transfer 76 (2016) 98-107. https://doi.org/10.1016/j.icheatmasstransfer.2016.04.028.
[15] L. Zhang, A. Zhang, Y. Jing, P. Qu, Z. Wu, J. Phys. Chem. C 125 (2021) 13590-13600. https://pubs.acs.org/doi/abs/10.1021/acs.jpcc.1c02014.
[16] M. Sheikholeslami, S.A. Shehzad, Z. Li, Int. J. Heat Mass Transfer 125 (2018) 375-386. https://doi.org/10.1016/j.ijheatmasstransfer.2018.04.076.
[17] Y. Guo, T. Zhang, D. Zhang, Q. Wang, Int. J. Heat Mass Transfer 117 (2018) 280-286. https://doi.org/10.1016/j.ijheatmasstransfer.2017.09.091.
[18] H. Xie, Z. Zhao, J. Zhao, H. Gao, Chin. J. Chem. Eng. 24 (2016) 331-338. https://doi.org/10.1016/j.cjche.2015.11.024.
[19] P. Bose, D. Deb, S. Bhattacharya, J. Power Sources 406 (2018) 176-184. https://doi.org/10.1016/j.jpowsour.2018.10.050.
[20] B. Tang, K.H. Row, Monatsh. Chem. 144 (2013) 1427-1454. https://doi.org/10.1007/s00706-013-1050-3
[21] T.H. Ibrahim, M.A. Sabri, N.A. Jabbar, P. Nancarrow, F.S. Mjalli, I. AlNashef, Molecules 25 (2020). https://doi.org/10.3390/molecules25173816.
[22] V. Agieienko, R. Buchner, J. Chem. Eng. Data 66 (2021) 780-792. https://doi.org/10.1021/je800468h.
[23] A.T. Celebi, T.J.H. Vlugt, O.A. Moultos, Mol. Phys. 119 (2021). https://doi.org/10.1080/00268976.2021.1876263.
[24] W. Shi, X. Chen, XWang, J. Mol. Liq. 395 (2024) 780-792. https://doi.org/10.1016/j.molliq.2023.123852
[25] C. Liu, Y. Yan, W. Sun, X. Shi, N. Shi, Y. Huo, J. Zhao, Z. Said, M. Sharifpur, J. Mol. Liq. 356 (2022) p.119020. https://doi.org/10.1016/j.molliq.2022.119020
[26] X. Chen, J. Jiang, F. Yan, S. Tian, K. Li, RSC Adv. 4 (2014) 8703-8710. https://doi.org/10.1039/C3RA47018K.
[27] I. Kumar, S.R. Rao, S.P. DilliBabu, K.S. Reddy, P.N. Reddy, M. Alam. S. Halder, H.A. Kumar, AIP Conf. Proc. 3267 (2025) p. 020302. https://doi.org/10.1063/5.0264786
[28] B. Vijayakumar, N. Ahalya, V. Venkatesan, J. Kamalakannan, Shubhajit Halder, Kumar Pratyush, AIP Conf. Proc. 69 (2022) 1005-1009. https://doi.org/10.1016/j.matpr.2022.07.462
[29] E. Rafiee, S. Shahebrahimi, M. Feyzi, M. Shaterzadeh, Int. Nano Lett. 2 (2012) 2-8. https://doi.org/10.1186/2228-5326-2-29.
[30] S.P. Manikandan, R. Baskar, Chem. Ind. Chem. Eng. Q. 27 (2021) 15-20. https://doi.org/10.2298/CICEQ191220020P.
[31] S.P. Manikandan, R. Baskar, Chem. Ind. Chem. Eng. Q. 27 (2021) 177-187. https://doi.org/10.2298/CICEQ200504036P.
[32] D. Wenzel, A. Górak, Chem. Eng. J. (Amsterdam, Neth.) 345(2018) 492-506. https://doi.org/10.1016/j.cej.2018.03.109
Click or tap here to enter text.

PERIASAMY MANIKANDAN
SRINIVASAN
JAYABALAN JAYABHARATHI

Department of Chemical Engineering, Kongu Engineering College, India

EKSPERIMENTALNA ISPITIVANJA PRIMENOM NENJUTNOVSKOG NANOFLUIDA SIO_2-VODA-EUTEKTIČKI RASTVARAČ U PLOČASTOM IZMENJIVAČU TOPLOTE

Pločasti izmenjivač toplote predstavlja jedan od najmanjih i najefikasnijih tipova izmenjivača toplote dostupnih na tržištu. Cilj ovog eksperimenta bio je da se proceni učinak smeše eutektičkog rastvarača i vode kao bazne tečnosti u pločastom izmenjivaču toplote. U okviru ove studije, nanočestice silicijum-dioksida (SiO_2) sintetisane su iz bagaze šećerne trske i pirinčane ljuske primenom sol-gel metode. Nanočestice SiO_2 korišćene su u različitim zapreminskim udelima (0,15; 0,3; 0,45; 0,6 i 0,75 vol.%) u baznoj tečnosti koja se sastojala od 15 vol.% eutektičkog rastvarača i 85 vol.% vode, radi pripreme nanofluida.Ispitivanja prenosa toplote sprovedena su pri tri različite temperature (323, 333 i 343 K), uz promenljive protoke (od 2 do 8 L/min) i različite koncentracije nanočestica (0,15-0,75 %). Dobijeni rezultati pokazuju značajno povećanje ukupnog koeficijenta prenosa toplote usled kombinovanog dejstva SiO_2 nanočestica i bazne tečnosti na bazi eutektičkog rastvarača i vode. Uočeno je da primena SiO_2/eutektički rastvarač-voda nanofluida može znatno smanjiti temperaturni gradijent u izmenjivaču toplote i poboljšati njegove performanse. Maksimalna vrednost ukupnog koeficijenta prenosa toplote iznosila je 3162,5 W/m²K pri zapreminskom udelu nanočestica od 0,6 %, protoku od 8 L/min i temperaturi od 343 K.

NAUČNI RAD

Ključne reči: bazna tečnost, eutektički rastvarač, prenos toplote, nenjutnovski nanofluid, pločasti izmenjivač toplote, SiO_2.